HHS Public Access

Author manuscript

Bioconjug Chem. Author manuscript; available in PMC 2019 May 31.

Published in final edited form as:

Bioconjug Chem. 2018 July 18; 29(7): 2161–2169. doi:10.1021/acs.bioconjchem.8b00285.

In Vivo Translation of Peptide-Targeted Drug Delivery Systems Discovered by Phage Display

Maureen R. Newman[†,§] and **Danielle S. W. Benoit**[*,†,‡,§]

[†]Biomedical Engineering, University of Rochester, Rochester, New York 14627, United States

[‡]Chemical Engineering, University of Rochester, Rochester, New York 14627, United States

[§]Center for Musculoskeletal Research, Department of Orthopaedics, University of Rochester Medical Center, Rochester, New York 14642, United States

Abstract

Therapeutic compounds with narrow therapeutic windows and significant systemic side effects benefit from targeted drug delivery strategies. Peptide-protein interactions are often exploited for targeting, with phage display a primary method to identify high-affinity peptide ligands that bind cell surface and matrix bound receptors preferentially expressed in target tissues. After isolating and sequencing high-binding phages, peptides are easily synthesized and chemically modified for incorporation into drug delivery systems, including peptide-drug conjugates, polymers, and nanoparticles. This review describes the phage display methodology to identify targeting peptide sequences, strategies to functionalize drug carriers with phage-derived peptides, specific examples of drug carriers with *in vivo* translation, and limitations and future applications of phage display to drug delivery.

Graphical Abstract:

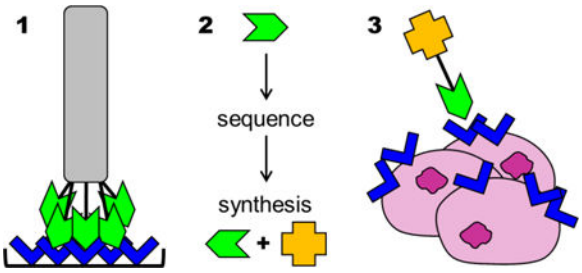

Phage display is used to identify peptides that bind target molecules, such as cell receptors expressed in diseased tissues, for generating targeted drug delivery systems.

Motivation

Drug delivery strategies are designed to address challenges associated with drug bioavailability, stability, solubility, and toxicity, as well as physiological barriers to cellular

* benoit@bme.rochester.edu.

entry.[1–3] Compounds with narrow therapeutic indices are particularly well-suited for administration by targeted drug delivery systems to avoid off-target effects in healthy tissues.[4] Early drug targeting systems exploited antibody-functionalized liposomes to enhance cell uptake and reduce systemic off-target accumulation.[1, 5] Recent efforts focus on peptides as targeting ligands, which can exhibit homology to antibodies and other native proteins, but are more economical and reproducible and are less likely to induce an immune response.[6, 7]

This review focuses on targeting peptides specifically identified through phage display, as the process can be used to screen against a range of targets such as whole cells or proteins to produce targeting ligands with affinities in the nanomolar range.[8, 9] Phage display is a multi-step selection and amplification process in which a random pool of 10^9-10^{10} random peptide sequences, each 7–12 amino acids long, is narrowed in as few as 3 rounds over a span of weeks.[10] This review describes the phage display process, highlights examples of phage display in targeted drug delivery, acknowledges limitations to phage display, and provides perspective on future applications of phage display in drug delivery.

Phage Display

Targeting peptides are often isolated via phage display. Bacteriophages, or more colloquially "phages," are viruses that infect and replicate within a host bacterium. Phages' proteins are surrounded by their encoding DNA, directly linking phenotype to genotype.[9] The first, and now most commonly used, phage for screening peptides libraries is the filamentous M13 bacteriophage; others include T4, T7, and λ phages.[11–13] DNA sequences can be inserted into a virus without disrupting normal function, leading to synthesis of the encoded peptide on the surface of the virus.[9] In Smith's seminal report, foreign DNA fragments were inserted into Gene III of M13 phage, resulting in expression of a foreign peptide on the pIII minor coat protein.[11] Typically, five peptide clones display the N-terminus of the foreign peptide, and the C-terminus is connected to the rest of pIII buried within the virion.[9] The display of only five peptides limits confounding multivalent effects, unlike modification of Gene VIII, which can result in up to 2700 copies of peptides displayed on pVIII major coat proteins.[14] The significant avidity of multicopy pVIII phage display libraries may overshadow relatively weak affinity of a single peptide clone.[9, 13] In other words, target binding of a low-affinity peptide causes neighboring low-affinity peptides to bind to the target, yielding a higher functional affinity (avidity) than the sum of individual peptides.[15, 16] The contribution of avidity can be measured using techniques such as isothermal calorimetry or surface plasmon resonance (SPR) spectroscopy. Avidity effects are minimized by reducing the number of displayed peptide clones via phages (pVIII or pIII) with both wild-type and recombinant genes.[17]

The process of phage display begins with generating a random peptide library (Figure 1A). Oligonucleotides $(NNK)_x(GGC)_y$ are inserted upstream of wild-type Gene III. Each "NNK" is a codon, where "N" is any nucleotide (A, C, G, or T) and "K" is usually either G or T to limit the number of possible codons.[13, 18] This yields 32 different codons that translate into "x" amino acids in the displayed peptide, and "$(GGC)_y$" translates into "y" glycine spacers between foreign peptide and pIII. It is noted that this method may not generate phages displaying every possible amino acid combination, as there is bias against amino acids with

only one codon, and some sequences may interfere with normal coat protein folding.[9, 18, 19] After generating a library, phages are exposed to immobilized molecular probes ranging from small molecules to proteins to whole cells in a process known as panning.[12] The method of panning is a multi-step process described in detail by Kay *et al.* and Freund *et al.*[13, 20] Briefly, the target is immobilized and phages are introduced in solution (Figure 1B). Unbound phages are washed away, and bound phages are stripped from the target using acidic, basic, or denaturing conditions. Recovered M13 phages are infected into *E. coil* to amplify (Figure 1D), and the series repeats for a chosen number of rounds.[14] Sequencing the DNA of phages after the final selection round identifies high-binding peptide sequences (Figure 1E).[9] For example, a random hexapeptide library of 3×10^8 phages was panned against 3-E7 monoclonal antibodies, resulting in 51 high-binding peptide sequences after three rounds of selection and amplification.[18] The antibody 3-E7 is specific to β-endorphin, which has an N-terminus beginning with Tyr-Gly-Gly-Phe, and 94% of the recovered phages displayed peptides beginning with Tyr-Gly. This highlights the ability of phage display to identify specific epitopes out of a highly diverse library.[21]

More robust phage selection has been achieved through parallel *in vitro* and *in vivo* screens. A thorough *in vitro* and *in vivo* phage display selection process by Whitney *et al.* identified tumor-targeting peptides.[22] In this study, hexahistidine-tagged phages (Figure 1A) were mixed with liver, kidney, and tumor extracts to identify sequences that were cleaved by only tumor enzymes (Figure 1B). The positively selected phages, which were those cleaved by tumor extracts but not liver and kidney extracts, were amplified and screened a total of six rounds (Figure 1D). In parallel, the library was injected into a transgenic breast cancer murine model, and cleaved phages were isolated from tumor extracts (Figure 1C). The recovered phages were amplified and injected into additional tumor-bearing mice for a total of 15 rounds (Figure 1D). One amino acid sequence, RLQLKL, was identified in both *in vitro* and *in vivo* screens. Further investigation demonstrated the utility of the peptide as an imaging agent for primary and metastatic tumors.[22]

Applications of Phage Display to Targeted Drug Delivery Systems

A wide variety of targeting peptide sequences have been identified through phage display. From the perspective of targeted drug delivery, cell receptors and extracellular matrix proteins that are specific to or enhanced by diseased tissues are used as bait.[23] Delivery systems functionalized with these targeting peptides are designed to preferentially distribute to target tissues upon systemic administration, limiting off-target carrier accumulation and adverse drug effects. Classes of drug delivery systems discussed in this review are highlighted in Figure 2 and include monovalent/multivalent peptide-drug conjugates, peptide-polymer-drug conjugates, monovalent/multivalent peptide-liposome conjugates, and peptide-micelle conjugates. Specific examples of chemical strategies to incorporate targeting peptides into delivery systems and applications that highlight the benefits of each system are summarized in Tables 1–2.

Peptide conjugates

Phage display has identified bioactive peptides with intrinsic targeting ability, but these peptides are uncommon. Frequently, various small molecules exhibit therapeutic potential, but many have poor pharmacokinetic profiles. These molecules can be combined with phage-derived peptides to form peptide-drug conjugates (Figure 2A) to realize their potential. Consideration must be given to the linkage between peptides and drugs to prevent binding interference or drug inactivation. Often, the affinities of synthetic peptides are orders of magnitude lower than phages, motivating the synthesis of multivalent peptide conjugates (Figure 2B) and multivalent peptide-polymer conjugates (Figure 2C). A summary of studies investigating bioactive targeting peptides and peptide-drug conjugates is given in Table 1.

Bioactive targeting peptides

Peptides alone can exhibit inherent therapeutic effects. A common characteristic of the bioactive peptides summarized in Table 1 is that the sequences contain two cysteine amino acids that form disulfide bonds and induce cyclicization. The cyclic structure is vital to function; for example, cyclic CTTHWGFTLC peptides specifically inhibited the enzymatic activity of both gelatinases, but linear peptides did not.[24] This is likely due to the structural constraints cyclicization places on a peptide, which facilitates proper amino acid orientation to bind to target epitopes.[49] Cyclic peptides also exhibit greater serum stability than their linear counterparts.[50] Of note, not all cyclic peptides are bioactive, as the control cyclic peptide GACVFSIAHECGA used by Arap *et al.* showed no tumor homing or activity.[30] An advantage of bioactive targeting peptides is the simplicity of synthesis, as solid-phase peptide synthesis and recombinant DNA technology are easily accessible methods. However, peptides are less than 10 kDa and freely filtered by the kidneys, leading to low plasma half-lives and limited tissue residence time.[51]

Monovalent peptide conjugates

Peptide conjugation to small molecules with poor pharmacokinetics enhances target tissue accumulation. A common peptide-drug conjugation route employs carbodiimide chemistry to functionalize the N- or C-termini of peptides with small molecules that contain amine or carboxylic acid functionalities, such as the chemotherapeutic doxorubicin (Dox)[30], or protein therapeutics with poor intrinsic target tissue distribution. In the case of protein and peptide therapeutics, it is also possible to synthesize the entire peptide-drug conjugate in one step.[31] However, a limitation to phage display is that synthesized peptides often exhibit affinities orders of magnitude lower (*i.e.* dissociation constants (K_D) orders of magnitudes higher) when avidity effects are removed, and monovalent peptide conjugates may not provide efficient target tissue distribution.

Multivalent peptide conjugates

Multivalent peptides are more akin to phage displays and antibodies, both of which exhibit avidity effects that yield affinity in the nanomolar or picomolar range.[16, 52] Avidity effects seem to be significant for multivalent peptide conjugates with four or more peptides copies.[36, 53] The benefit of multivalent peptide conjugates relative to monovalent peptide conjugates is highlighted by the peptide HVWMQAPGGG, which was identified to have

high affinity for collagen using phage display.[54] Analysis of binding kinetics by SPR spectroscopy identified rapid association and dissociation of the peptide, resulting in K_D of only 61 μM. When the peptide was incorporated into a fifth-generation dendrimer, affinity was dramatically increased 100-fold to 550 nM.

Although peptide-targeted dendrimers provide versatility in drug delivery by enabling hydrophobic drug encapsulation, covalent drug conjugation, and siRNA complexation,[55, 56] a major limitation is the cationic charge of dendrimers that can cause cytotoxicity due to membrane disruption.[55] Surface engineering strategies have improved the cytocompatibility of dendrimers by masking cationic charges,[57] but upon injection, dendrimers tend to aggregate and accumulate in the lungs.[58] While this characteristic may be useful for drug delivery to the lungs, it is inefficient for delivery to other tissues and may cause toxicity. As a result, there are limited clinical applications of dendrimers as drug delivery vehicles.[59]

Multivalent polymer conjugates

Underscored by multivalent peptide-drug conjugates, multi-peptide incorporation into a carrier enables much greater binding avidity versus singular peptide binding affinity. However, when peptides are hydrophobic, aggregation may obscure binding and poor solubility can hinder applicability to drug delivery.[60] Copolymer conjugates enable functionalization of a core hydrophilic polymer, such as commonly used poly(ethylene glycol) (PEG) or *N*-(2-hydroxypropyl)methacrylamide (HPMA), with targeting peptides. As an added advantage, copolymers can also incorporate multiple drug molecules to enhance drug payload (Figure 2C). Two methods are employed for peptide functionalization: peptide incorporation during polymerization and post-polymerization peptide incorporation. Based on monomer functionalities and reactivity ratios, gradient and uniform peptide incorporation can be achieved. A study comparing these two polymer architectures identified greater, but less stable, target binding of gradient copolymers with increasing peptide content, but greater binding stability with random copolymers above 15% percent peptide content.[48] *In vivo*, the fracture-targeted random copolymers persisted in bone for at least one week, whereas gradient copolymers were cleared, demonstrating that the two-step synthesis scheme is more promising for fracture targeting.

One benefit to post-polymerization functionalization is the ability to use polymer functionalities to incorporate both peptides and drugs. A prostate cancer cell-targeting HPMA copolymer was designed using *N*-methacryloyl-glycylglycine-4-nitrophenyl ester (MA-GG-ONp) as a comonomer.[61] The ONp functionality was used to facilitate peptide incorporation, and unreacted ONp groups were reacted with hydrazine hydrate to facilitate doxorubicin incorporation. The use of the hydrazine bond between the polymer and DOX enabled pH-responsive release and resulted in significant anti-proliferative activity in prostate cancer cells relative to unconjugated free doxorubicin.[61] However, a limitation to multivalent polymer conjugates as drug delivery systems is the need to functionalize drugs for incorporation if no functional groups, such as the amine in doxorubicin, exist.

Multivalent Nanoparticles

Some therapeutic compounds lack functionalities for conjugation and are difficult to deliver with polymer conjugates. Nanoparticles (NP) can be used to deliver these compounds: specifically, liposomes for both hydrophobic and hydrophilic molecules (Figure 2D) and micelles for hydrophobic molecules (Figure 2E). NPs are colloidal suspensions of amphiphilic polymers and are inherently multivalent. Careful polymer selection provides functionalities amenable to peptide incorporation, either pre- or post-particle assembly. Peptide conjugation after NP assembly may lead to a more even distribution of peptides across the particle surface but may limit accessibility of functional groups and cause poor functionalization efficiency. Peptide conjugation to polymers before NP assembly provides greater control over degree of functionalization but does not necessarily homogeneously display peptides, as aggregates may form “islands” of peptide on the particle surface. Examples of both strategies are summarized in Table 2.

Multivalent peptide-nanoparticle (NP) conjugates

The array of commercially available reagents, well documented synthesis schemes, and flexibility of drug loading has made peptide-targeted NPs a common drug delivery approach. The approach is particularly suited to cancer therapeutics because the ~100–200 nm sizes of liposomes and micelles enable extravasation and passive accumulation in leaky tumor vasculature via the enhanced permeability and retention (EPR) effect.[81] It is also suited to conditions with an inflammatory component, such as fractures.[62] However, there is room for improvement, as some systems with active peptide-targeting exhibit only two-fold increased target accumulation[62] and achieve similar end point outcomes[76] as untargeted systems.

A method of improving NP targeting is to incorporate two different targeting peptides.[64, 82] One peptide could be targeted to proteins within the extracellular microenvironment, and the other could be targeted to receptors on the surface of target cells. This strategy may mitigate off-target cell activation, as phage-derived peptides can bind to more than their intended target receptors.[83] Targeting by multivalent NPs can be further enhanced by multivalent peptide display on multivalent NPs (Figure 2D2). Monomeric and tetrameric peptides were incorporated into liposomal NPs to investigate the effects of both peptide valence and NP valence on binding.[84] Liposomes bearing similar numbers of peptides showed that tetrameric peptides enhance cell uptake relative to monomeric and that increased tetrameric peptide density further increased specificity, suggesting multivalence is beneficial.[84]

Perspective

Phage display is a powerful technique to identify targeting peptides, but it comes with limitations. False positives can arise through selection of phages bound to plastic substrates or blocking agents, as well as selection of phages that amplified due to propagation advantages.[85] Even a small difference (~10%) in growth rates or infectivity can disrupt the diversity of a phage library.[86] For example, the commercially available New England Biolab Ph.D.−7 phage display library, generated using a degenerate 7-mer library, produces clones enhanced with proline and depleted with cysteine, suggesting a propagation advantage to clones containing proline residues.[87] The heptapeptide HAIYPRH underscores this issue, as

it has been identified in at least 14 independent biopanning experiments and accounts for 0.26% of peptides that pass one round of selection and amplification.[87] Next generation sequencing (NGS), which has become more accessible with technological advancements, may address these concerns. NGS applied after each selection round may identify sequences with high target affinity that are not selected following amplification due to inferior infectivity or growth.[87, 88]

An interesting future direction in phage display technology is selective modification by non-standard amino acids[89] such as selenocysteine (Sec), the 21st amino acid. Although chemically related to cysteine (Cys), Sec has a sidechain pKa lower than that of Cys (~5 vs ~8) and is more nucleophilic at physiological pH (~7.4). This enables functionalization of the Sec thiol within the foreign phage sequence without affecting other coat proteins. Beech *et al.* employed this strategy to incorporate small molecule binders of one type of G protein-coupled receptor, the adenosine A_1 receptor, into phages.[90] The molecule, N^6-Octylaminoadenosine, retained affinity to A_1 receptors despite conjugation to phage by its primary amine; moreover, avidity effects led to a 14-fold lower EC_{50} in activating downstream Akt signaling. Similarly, Li *et al.* replaced the original disulfide bonds of a tumor-targeting peptide, Lyp-1, with diseleno bonds to increase serum stability and saw a reduction in the IC_{50} of liposomal doxorubicin that led to 75% tumor growth inhibition.[91] An application of this approach would be to perform a biopan of peptide(Sec)-displaying phages against a target cell type to identify cell-specific targeting peptides before modifying the selected phages with small molecule agonists intended to act on the target cells. Then, either a synthetic peptide(Sec)-drug conjugate or the modified coat protein[92] could be used for cell-specific small molecule delivery.

Conclusions

Phage display has progressed from a tool for cloning genes[11] to a tool for developing targeted drug delivery systems. The versatility of panning against any molecule, protein, or cell enables the design of targeting peptides that are highly specific to target tissues. After identifying specific peptides, various chemistries are used to incorporate peptides into multivalent drug conjugates that exhibit high target affinity. Careful experimental design and post-hoc analyses are necessary to mitigate false positives that can arise during the processes of selection and amplification. Phage display technology is highly accessible with the diverse commercial availability of random peptide libraries, leading to successful applications in targeted drug delivery.

Acknowledgements

This work was supported by the National Science Foundation (NSF) *CBET*-1450987 and DGE-1419118.

References

(1). Davis SS, Hunneyball IM, Illum L, Ratcliffe JH, Smith A, and Wilson CG (1985) Recent advances in the use of microspheres for targeted therapy. Drugs Exp Clin Res 11, 633–40. [PubMed: 3880050]

(2). Ye C, and Chi H (2018) A review of recent progress in drug and protein encapsulation: Approaches, applications and challenges. Mater Sci Eng C Mater Biol Appl 83, 233–246. [PubMed: 29208283]

(3). Tyagi P, and Subramony JA (2018) Nanotherapeutics in oral and parenteral drug delivery: Key learnings and future outlooks as we think small. J Control Release 272, 159–168. [PubMed: 29355619]

(4). Papachristos A, Pippa N, Demetzos C, and Sivolapenko G (2016) Antibody-drug conjugates: a mini-review. The synopsis of two approved medicines. Drug Deliv 23, 1662–6. [PubMed: 25625494]

(5). Papahadjopoulos D, Heath T, Bragman K, and Matthay K (1985) New methodology for liposome targeting to specific cells. Ann N Y Acad Sci 446, 341–8. [PubMed: 2861775]

(6). Sheu TJ, Schwarz EM, O'Keefe RJ, Rosier RN, and Puzas JE (2002) Use of a phage display technique to identify potential osteoblast binding sites within osteoclast lacunae. J Bone Miner Res 17, 915–22. [PubMed: 12009023]

(7). McGuire MJ, Samli KN, Johnston SA, and Brown KC (2004) In vitro selection of a peptide with high selectivity for cardiomyocytes in vivo. J Mol Biol 342, 171–82. [PubMed: 15313615]

(8). Uchiyama F, Tanaka Y, Minari Y, and Tokui N (2005) Designing scaffolds of peptides for phage display libraries. J Biosci Bioeng 99, 448–56. [PubMed: 16233816]

(9). Rodi DJ, and Makowski L (1999) Phage-display technology--finding a needle in a vast molecular haystack. Curr Opin Biotechnol 10, 87–93. [PubMed: 10047512]

(10). Koscielska K, Kiczak L, Kasztura M, Wesolowska O, and Otlewski J (1998) Phage display of proteins. Acta Biochim Pol 45, 705–20. [PubMed: 9918498]

(11). Smith GP (1985) Filamentous fusion phage: novel expression vectors that display cloned antigens on the virion surface. Science 228, 1315–7. [PubMed: 4001944]

(12). Bazan J, Calkosinski I, and Gamian A (2012) Phage display--a powerful technique for immunotherapy: 1. Introduction and potential of therapeutic applications. Hum Vaccin Immunother 8, 1817–28. [PubMed: 22906939]

(13). Kay BK, Kasanov J, and Yamabhai M (2001) Screening phage-displayed combinatorial peptide libraries. Methods 24, 240–6. [PubMed: 11403573]

(14). Azzazy HM, and Highsmith WE Jr. (2002) Phage display technology: clinical applications and recent innovations. Clin Biochem 35, 425–45. [PubMed: 12413604]

(15). Vauquelin G, and Charlton SJ (2013) Exploring avidity: understanding the potential gains in functional affinity and target residence time of bivalent and heterobivalent ligands. Br J Pharmacol 168, 1771–85. [PubMed: 23330947]

(16). Rudnick SI, and Adams GP (2009) Affinity and avidity in antibody-based tumor targeting. Cancer Biother Radiopharm 24, 155–61. [PubMed: 19409036]

(17). (1993) Surface display and peptide libraries. Cold Spring Harbor Laboratory, April 4–7, 1992. Proceedings. Gene 128, 1–144. [PubMed: 8508950]

(18). Cwirla SE, Peters EA, Barrett RW, and Dower WJ (1990) Peptides on phage: a vast library of peptides for identifying ligands. Proc Natl Acad Sci U S A 87, 6378–82. [PubMed: 2201029]

(19). Ryvkin A, Ashkenazy H, Weiss-Ottolenghi Y, Piller C, Pupko T, and Gershoni JM (2018) Phage display peptide libraries: deviations from randomness and correctives. Nucleic Acids Res

(20). Freund NT, Enshell-Seijffers D, and Gershoni JM (2009) Phage display selection, analysis, and prediction of B cell epitopes. Curr Protoc Immunol Chapter 9, Unit 9 8.

(21). Scott JK, and Smith GP (1990) Searching for peptide ligands with an epitope library. Science 249, 386–90. [PubMed: 1696028]

(22). Whitney M, Crisp JL, Olson ES, Aguilera TA, Gross LA, Ellies LG, and Tsien RY (2010) Parallel in vivo and in vitro selection using phage display identifies protease-dependent tumor-targeting peptides. J Biol Chem 285, 22532–41. [PubMed: 20460372]

(23). Newman MR, and Benoit DS (2016) Local and targeted drug delivery for bone regeneration. Curr Opin Biotechnol 40, 125–132. [PubMed: 27064433]

(24). Koivunen E, Arap W, Valtanen H, Rainisalo A, Medina OP, Heikkila P, Kantor C, Gahmberg CG, Salo T, Konttinen YT, et al. (1999) Tumor targeting with a selective gelatinase inhibitor. Nat Biotechnol 17, 768–74. [PubMed: 10429241]

(25). Marchio S, Lahdenranta J, Schlingemann RO, Valdembri D, Wesseling P, Arap MA, Hajitou A, Ozawa MG, Trepel M, Giordano RJ, et al. (2004) Aminopeptidase A is a functional target in angiogenic blood vessels. Cancer Cell 5, 151–62. [PubMed: 14998491]

(26). Laakkonen P, Akerman ME, Biliran H, Yang M, Ferrer F, Karpanen T, Hoffman RM, and Ruoslahti E (2004) Antitumor activity of a homing peptide that targets tumor lymphatics and tumor cells. Proc Natl Acad Sci U S A 101, 9381–6. [PubMed: 15197262]

(27). Laakkonen P, Porkka K, Hoffman JA, and Ruoslahti E (2002) A tumor-homing peptide with a targeting specificity related to lymphatic vessels. Nat Med 8, 751–5. [PubMed: 12053175]

(28). Xie X, Kerrigan JE, Minko T, Garbuzenko O, Lee KC, Scarborough A, Abali EE, Budak-Alpdogan T, Johnson-Farley N, Banerjee D, et al. (2013) Antitumor and modeling studies of a penetratin-peptide that targets E2F-1 in small cell lung cancer. Cancer Biol Ther 14, 742–51. [PubMed: 23792570]

(29). Xie X, Bansal N, Shaik T, Kerrigan JE, Minko T, Garbuzenko O, Abali EE, Johnson-Farley N, Banerjee D, Scotto KW, et al. (2014) A novel peptide that inhibits E2F transcription and regresses prostate tumor xenografts. Oncotarget 5, 901–7. [PubMed: 24658650]

(30). Arap W, Pasqualini R, and Ruoslahti E (1998) Cancer treatment by targeted drug delivery to tumor vasculature in a mouse model. Science 279, 377–80. [PubMed: 9430587]

(31). Curnis F, Sacchi A, Borgna L, Magni F, Gasparri A, and Corti A (2000) Enhancement of tumor necrosis factor alpha antitumor immunotherapeutic properties by targeted delivery to aminopeptidase N (CD13). Nat Biotechnol 18, 1185–90. [PubMed: 11062439]

(32). Jin W, Qin B, Chen Z, Liu H, Barve A, and Cheng K (2016) Discovery of PSMA-specific peptide ligands for targeted drug delivery. Int J Pharm 513, 138–147. [PubMed: 27582001]

(33). Cieslewicz M, Tang J, Yu JL, Cao H, Zavaljevski M, Motoyama K, Lieber A, Raines EW, and Pun SH (2013) Targeted delivery of proapoptotic peptides to tumor-associated macrophages improves survival. Proc Natl Acad Sci U S A 110, 15919–24. [PubMed: 24046373]

(34). Elayadi AN, Samli KN, Prudkin L, Liu YH, Bian A, Xie XJ, Wistuba II, Roth JA, McGuire MJ, and Brown KC (2007) A peptide selected by biopanning identifies the integrin alphavbeta6 as a prognostic biomarker for nonsmall cell lung cancer. Cancer Res 67, 5889–95. [PubMed: 17575158]

(35). Oyama T, Sykes KF, Samli KN, Minna JD, Johnston SA, and Brown KC (2003) Isolation of lung tumor specific peptides from a random peptide library: generation of diagnostic and cell-targeting reagents. Cancer Lett 202, 219–30. [PubMed: 14643452]

(36). Li S, McGuire MJ, Lin M, Liu YH, Oyama T, Sun X, and Brown KC (2009) Synthesis and characterization of a high-affinity {alpha}v{beta}6-specific ligand for in vitro and in vivo applications. Mol Cancer Ther 8, 1239–49. [PubMed: 19435868]

(37). Liu J, Liu J, Chu L, Wang Y, Duan Y, Feng L, Yang C, Wang L, and Kong D (2010) Novel peptide-dendrimer conjugates as drug carriers for targeting nonsmall cell lung cancer. Int J Nanomedicine 6, 59–69. [PubMed: 21289982]

(38). Lee SM, Lee EJ, Hong HY, Kwon MK, Kwon TH, Choi JY, Park RW, Kwon TG, Yoo ES, Yoon GS, et al. (2007) Targeting bladder tumor cells in vivo and in the urine with a peptide identified by phage display. Mol Cancer Res 5, 11–9. [PubMed: 17259343]

(39). Sarangthem V, Cho EA, Yi A, Kim SK, Lee BH, and Park RW (2018) Application of Bld-1-Embedded Elastin-Like Polypeptides in Tumor Targeting. Sci Rep 8, 3892. [PubMed: 29497090]

(40). Hong HY, Lee HY, Kwak W, Yoo J, Na MH, So IS, Kwon TH, Park HS, Huh S, Oh GT, et al. (2008) Phage display selection of peptides that home to atherosclerotic plaques: IL-4 receptor as a candidate target in atherosclerosis. J Cell Mol Med 12, 2003–14. [PubMed: 19012727]

(41). Sarangthem V, Cho EA, Bae SM, Singh TD, Kim SJ, Kim S, Jeon WB, Lee BH, and Park RW (2013) Construction and application of elastin like polypeptide containing IL-4 receptor targeting peptide. PLoS One 8, e81891. [PubMed: 24339977]

(42). Simberg D, Duza T, Park JH, Essler M, Pilch J, Zhang L, Derfus AM, Yang M, Hoffman RM, Bhatia S, et al. (2007) Biomimetic amplification of nanoparticle homing to tumors. Proc Natl Acad Sci U S A 104, 932–6. [PubMed: 17215365]

(43). Lempens EH, Merkx M, Tirrell M, and Meijer EW (2011) Dendrimer display of tumor-homing peptides. Bioconjug Chem 22, 397–405. [PubMed: 21261269]

(44). Martens CL, Cwirla SE, Lee RY, Whitehorn E, Chen EY, Bakker A, Martin EL, Wagstrom C, Gopalan P, Smith CW, et al. (1995) Peptides which bind to E-selectin and block neutrophil adhesion. J Biol Chem 270, 21129–36. [PubMed: 7545665]

(45). Shamay Y, Raviv L, Golan M, Voronov E, Apte RN, and David A (2015) Inhibition of primary and metastatic tumors in mice by E-selectin-targeted polymer-drug conjugates. J Control Release 217, 102–12. [PubMed: 26297207]

(46). An P, Lei H, Zhang J, Song S, He L, Jin G, Liu X, Wu J, Meng L, Liu M, et al. (2004) Suppression of tumor growth and metastasis by a VEGFR-1 antagonizing peptide identified from a phage display library. Int J Cancer 111, 165–73. [PubMed: 15197767]

(47). Shamay Y, Golan M, Tyomkin D, and David A (2016) Assessing the therapeutic efficacy of VEGFR-1-targeted polymer drug conjugates in mouse tumor models. J Control Release 229, 192–199. [PubMed: 27001892]

(48). Newman MR, Russell SG, Schmitt CS, Marozas IA, Sheu TJ, Puzas JE, and Benoit DSW (2018) Multivalent Presentation of Peptide Targeting Groups Alters Polymer Biodistribution to Target Tissues. Biomacromolecules 19, 71–84. [PubMed: 29227674]

(49). Millward SW, Fiacco S, Austin RJ, and Roberts RW (2007) Design of cyclic peptides that bind protein surfaces with antibody-like affinity. ACS Chem Biol 2, 625–34. [PubMed: 17894440]

(50). Ngambenjawong C, Gustafson HH, Pineda JM, Kacherovsky NA, Cieslewicz M, and Pun SH (2016) Serum Stability and Affinity Optimization of an M2 Macrophage-Targeting Peptide (M2pep). Theranostics 6, 1403–14. [PubMed: 27375788]

(51). Diao L, and Meibohm B (2013) Pharmacokinetics and pharmacokinetic-pharmacodynamic correlations of therapeutic peptides. Clin Pharmacokinet 52, 855–68. [PubMed: 23719681]

(52). Beirnaert E, Desmyter A, Spinelli S, Lauwereys M, Aarden L, Dreier T, Loris R, Silence K, Pollet C, Cambillau C, et al. (2017) Bivalent Llama Single-Domain Antibody Fragments against Tumor Necrosis Factor Have Picomolar Potencies due to Intramolecular Interactions. Front Immunol 8, 867. [PubMed: 28824615]

(53). Bastings MM, Helms BA, van Baal I, Hackeng TM, Merkx M, and Meijer EW (2011) From phage display to dendrimer display: insights into multivalent binding. J Am Chem Soc 133, 6636–41. [PubMed: 21473586]

(54). Helms BA, Reulen SW, Nijhuis S, de Graaf-Heuvelmans PT, Merkx M, and Meijer EW (2009) High-affinity peptide-based collagen targeting using synthetic phage mimics: from phage display to dendrimer display. J Am Chem Soc 131, 11683–5. [PubMed: 19642697]

(55). Patri AK, Kukowska-Latallo JF, and Baker JR Jr. (2005) Targeted drug delivery with dendrimers: comparison of the release kinetics of covalently conjugated drug and non-covalent drug inclusion complex. Adv Drug Deliv Rev 57, 2203–14. [PubMed: 16290254]

(56). Leiro V, Santos SD, and Pego AP (2017) Delivering siRNA with Dendrimers: In Vivo Applications. Curr Gene Ther 17, 105–119. [PubMed: 28494741]

(57). Jain K, Kesharwani P, Gupta U, and Jain NK (2010) Dendrimer toxicity: Let's meet the challenge. Int J Pharm 394, 122–42. [PubMed: 20433913]

(58). Khan OF, Zaia EW, Jhunjhunwala S, Xue W, Cai W, Yun DS, Barnes CM, Dahlman JE, Dong Y, Pelet JM, et al. (2015) Dendrimer-Inspired Nanomaterials for the in Vivo Delivery of siRNA to Lung Vasculature. Nano Lett 15, 3008–16. [PubMed: 25789998]

(59). Kannan RM, Nance E, Kannan S, and Tomalia DA (2014) Emerging concepts in dendrimer-based nanomedicine: from design principles to clinical applications. J Intern Med 276, 579–617. [PubMed: 24995512]

(60). Ngambenjawong C, and Pun SH (2017) Multivalent polymers displaying M2 macrophage-targeting peptides improve target binding avidity and serum stability. ACS Biomater Sci Eng 3, 2050–2053. [PubMed: 29430522]

(61). Pola R, Pechar M, Ulbrich K, and Fres AF (2007) Polymer-doxorubicin conjugate with a synthetic peptide ligand targeted on prostate tumor. J Bioact Compat Pol 22, 602–620.

(62). Wang Y, Newman MR, Ackun-Farmmer M, Baranello MP, Sheu TJ, Puzas JE, and Benoit DSW (2017) Fracture-Targeted Delivery of beta-Catenin Agonists via Peptide-Functionalized Nanoparticles Augments Fracture Healing. ACS Nano 11, 9445–9458. [PubMed: 28881139]

(63). Fukuta T, Asai T, Kiyokawa Y, Nakada T, Bessyo-Hirashima K, Fukaya N, Hyodo K, Takase K, Kikuchi H, and Oku N (2017) Targeted delivery of anticancer drugs to tumor vessels by use of liposomes modified with a peptide identified by phage biopanning with human endothelial progenitor cells. Int J Pharm 524, 364–372. [PubMed: 28359814]

(64). Loi M, Marchio S, Becherini P, Di Paolo D, Soster M, Curnis F, Brignole C, Pagnan G, Perri P, Caffa I, et al. (2010) Combined targeting of perivascular and endothelial tumor cells enhances anti-tumor efficacy of liposomal chemotherapy in neuroblastoma. J Control Release 145, 66–73. [PubMed: 20346382]

(65). Han Z, Fu A, Wang H, Diaz R, Geng L, Onishko H, and Hallahan DE (2008) Noninvasive assessment of cancer response to therapy. Nat Med 14, 343–9. [PubMed: 18297085]

(66). Lowery A, Onishko H, Hallahan DE, and Han Z (2011) Tumor-targeted delivery of liposome-encapsulated doxorubicin by use of a peptide that selectively binds to irradiated tumors. J Control Release 150, 117–24. [PubMed: 21075152]

(67). Li J, Feng L, Fan L, Zha Y, Guo L, Zhang Q, Chen J, Pang Z, Wang Y, Jiang X, et al. (2011) Targeting the brain with PEG-PLGA nanoparticles modified with phage-displayed peptides. Biomaterials 32, 4943–50. [PubMed: 21470674]

(68). Passarella RJ, Spratt DE, van der Ende AE, Phillips JG, Wu H, Sathiyakumar V, Zhou L, Hallahan DE, Harth E, and Diaz R (2010) Targeted nanoparticles that deliver a sustained, specific release of Paclitaxel to irradiated tumors. Cancer Res 70, 4550–9. [PubMed: 20484031]

(69). Chan JM, Zhang L, Tong R, Ghosh D, Gao W, Liao G, Yuet KP, Gray D, Rhee JW, Cheng J, et al. (2010) Spatiotemporal controlled delivery of nanoparticles to injured vasculature. Proc Natl Acad Sci U S A 107, 2213–8. [PubMed: 20133865]

(70). Pastorino F, Brignole C, Marimpietri D, Cilli M, Gambini C, Ribatti D, Longhi R, Allen TM, Corti A, and Ponzoni M (2003) Vascular damage and anti-angiogenic effects of tumor vessel-targeted liposomal chemotherapy. Cancer Res 63, 7400–9. [PubMed: 14612539]

(71). Pastorino F, Di Paolo D, Piccardi F, Nico B, Ribatti D, Daga A, Baio G, Neumaier CE, Brignole C, Loi M, et al. (2008) Enhanced antitumor efficacy of clinical-grade vasculature-targeted liposomal doxorubicin. Clin Cancer Res 14, 7320–9. [PubMed: 19010847]

(72). Garde SV, Forte AJ, Ge M, Lepekhin EA, Panchal CJ, Rabbani SA, and Wu JJ (2007) Binding and internalization of NGR-peptide-targeted liposomal doxorubicin (TVT-DOX) in CD13-expressing cells and its antitumor effects. Anticancer Drugs 18, 1189–200. [PubMed: 17893520]

(73). Liu JK, Lubelski D, Schonberg DL, Wu Q, Hale JS, Flavahan WA, Mulkearns-Hubert EE, Man J, Hjelmeland AB, Yu J, et al. (2014) Phage display discovery of novel molecular targets in glioblastoma-initiating cells. Cell Death Differ 21, 1325–39. [PubMed: 24832468]

(74). Zhang M, Chen X, Ying M, Gao J, Zhan C, and Lu W (2017) Glioma-Targeted Drug Delivery Enabled by a Multifunctional Peptide. Bioconjug Chem 28, 775–781. [PubMed: 27966896]

(75). Hofmeister LH, Lee SH, Norlander AE, Montaniel KR, Chen W, Harrison DG, and Sung HJ (2015) Phage-display-guided nanocarrier targeting to atheroprone vasculature. ACS Nano 9, 4435–46. [PubMed: 25768046]

(76). Oku N, Asai T, Watanabe K, Kuromi K, Nagatsuka M, Kurohane K, Kikkawa H, Ogino K, Tanaka M, Ishikawa D, et al. (2002) Anti-neovascular therapy using novel peptides homing to angiogenic vessels. Oncogene 21, 2662–9. [PubMed: 11965539]

(77). Chung J, Shim H, Kim K, Lee D, Kim WJ, Kang DH, Kang SW, Jo H, and Kwon K (2016) Discovery of novel peptides targeting pro-atherogenic endothelium in disturbed flow regions - Targeted siRNA delivery to pro-atherogenic endothelium in vivo. Sci Rep 6, 25636. [PubMed: 27173134]

(78). Joyce JA, Laakkonen P, Bernasconi M, Bergers G, Ruoslahti E, and Hanahan D (2003) Stage-specific vascular markers revealed by phage display in a mouse model of pancreatic islet tumorigenesis. Cancer Cell 4, 393–403. [PubMed: 14667506]

(79). Valetti S, Maione F, Mura S, Stella B, Desmaele D, Noiray M, Vergnaud J, Vauthier C, Cattel L, Giraudo E, et al. (2014) Peptide-functionalized nanoparticles for selective targeting of pancreatic tumor. J Control Release 192, 29–39. [PubMed: 24984010]

(80). Qian Y, Zha Y, Feng B, Pang Z, Zhang B, Sun X, Ren J, Zhang C, Shao X, Zhang Q, et al. (2013) PEGylated poly(2-(dimethylamino) ethyl methacrylate)/DNA polyplex micelles decorated with phage-displayed TGN peptide for brain-targeted gene delivery. Biomaterials 34, 2117–29. [PubMed: 23245924]

(81). Noguchi Y, Wu J, Duncan R, Strohalm J, Ulbrich K, Akaike T, and Maeda H (1998) Early phase tumor accumulation of macromolecules: a great difference in clearance rate between tumor and normal tissues. Jpn J Cancer Res 89, 307–14. [PubMed: 9600125]

(82). Kuo CH, Leon L, Chung EJ, Huang RT, Sontag TJ, Reardon CA, Getz GS, Tirrell M, and Fang Y (2014) Inhibition of atherosclerosis-promoting microRNAs via targeted polyelectrolyte complex micelles. J Mater Chem B 2, 8142–8153. [PubMed: 25685357]

(83). Li L, Orner BP, Huang T, Hinck AP, and Kiessling LL (2010) Peptide ligands that use a novel binding site to target both TGF-beta receptors. Mol Biosyst 6, 2392–402. [PubMed: 20890540]

(84). Gray BP, Li S, and Brown KC (2013) From phage display to nanoparticle delivery: functionalizing liposomes with multivalent peptides improves targeting to a cancer biomarker. Bioconjug Chem 24, 85–96. [PubMed: 23186007]

(85). Vodnik M, Zager U, Strukelj B, and Lunder M (2011) Phage display: selecting straws instead of a needle from a haystack. Molecules 16, 790–817. [PubMed: 21248664]

(86). Derda R, Tang SK, Li SC, Ng S, Matochko W, and Jafari MR (2011) Diversity of phage-displayed libraries of peptides during panning and amplification. Molecules 16, 1776–803. [PubMed: 21339712]

(87). t Hoen PA, Jirka SM, Ten Broeke BR, Schultes EA, Aguilera B, Pang KH, Heemskerk H, Aartsma-Rus A, van Ommen GJ, and den Dunnen JT (2012) Phage display screening without repetitious selection rounds. Anal Biochem 421, 622–31. [PubMed: 22178910]

(88). Georgieva Y, and Konthur Z (2011) Design and screening of M13 phage display cDNA libraries. Molecules 16, 1667–81. [PubMed: 21330956]

(89). Tian F, Tsao ML, and Schultz PG (2004) A phage display system with unnatural amino acids. J Am Chem Soc 126, 15962–3. [PubMed: 15584720]

(90). Beech J, Saleh L, Frentzel J, Figler H, Correa IR Jr., Baker B, Ramspacher C, Marshall M, Dasa S, Linden J, et al. (2015) Multivalent site-specific phage modification enhances the binding affinity of receptor ligands. Bioconjug Chem 26, 529–36. [PubMed: 25692462]

(91). Li C, Wang Y, Zhang X, Deng L, Zhang Y, and Chen Z (2013) Tumor-targeted liposomal drug delivery mediated by a diseleno bond-stabilized cyclic peptide. Int J Nanomedicine 8, 1051–62. [PubMed: 23515368]

(92). Bedi D, Musacchio T, Fagbohun OA, Gillespie JW, Deinnocentes P, Bird RC, Bookbinder L, Torchilin VP, and Petrenko VA (2011) Delivery of siRNA into breast cancer cells via phage fusion protein-targeted liposomes. Nanomedicine 7, 315–23. [PubMed: 21050894]

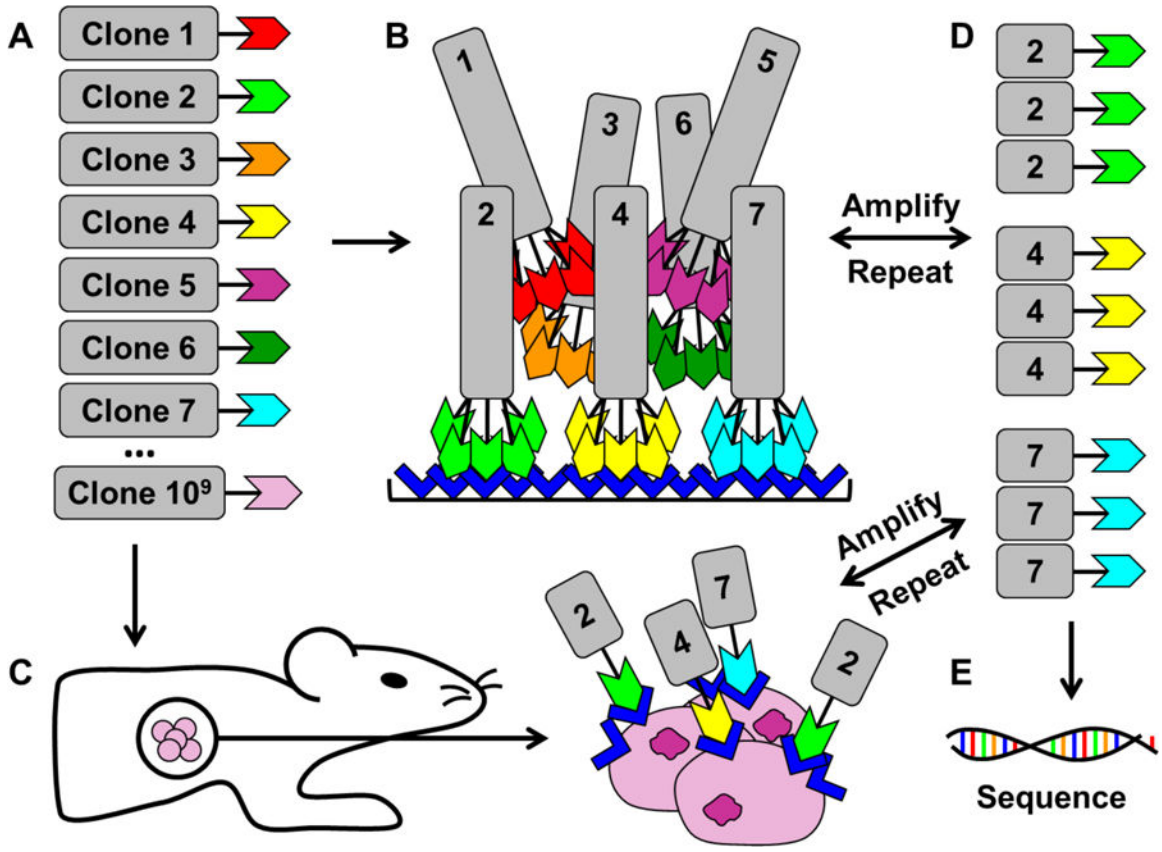

Figure 1.

Phage display methodology. A random library of clones (A) is panned *in vitro* (B) or *in vivo* (C) to identify target-bound phages. Phages are eluted from the target, amplified (D), and re-panned in multiple rounds of selection. Phages present in the final round of selection are sequenced to identify high-binding peptide clones (E).

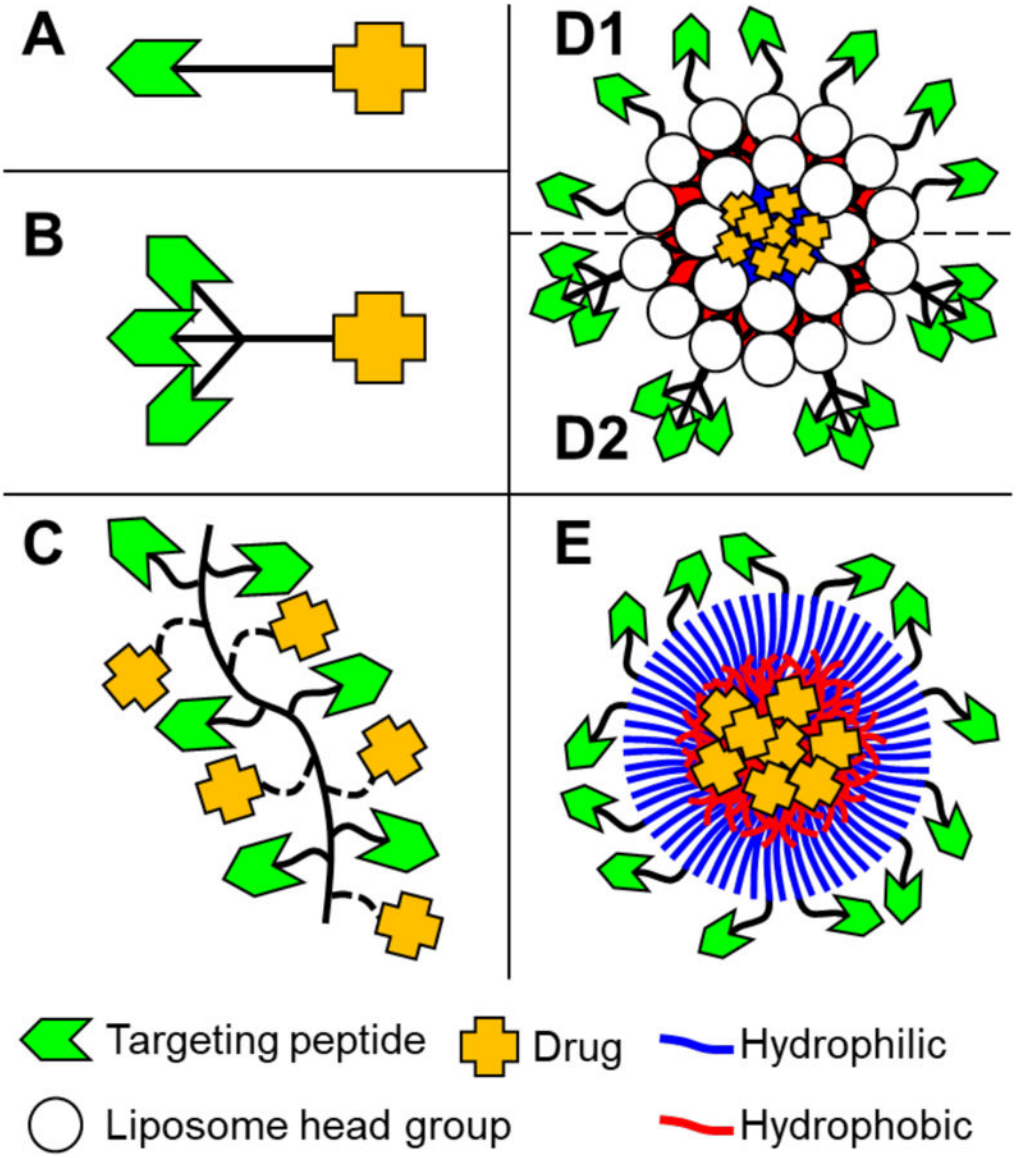

Figure 2.

Configurations of drug delivery systems with targeting ligands (green chevrons) and drug payloads (orange crosses). Highlighted are simple monovalent peptide-drug conjugates (A), multivalent peptide-drug conjugates (B), multivalent peptide-polymer-drug conjugates (C), monovalent (D1) and multivalent (D2) peptide-liposome conjugates, and peptide-micelle conjugates (E).

Table 1:

Summary of studies investigating phage display to design targeted peptide conjugates.

Indication	Target	Targeting Peptide	Result	Ref
Bioactive Targeting Peptides				
Kaposi's sarcoma xenograft in nude mice	Gelatinase B	CTTHWGFTLC	Inhibited endothelial and tumor cell migration *in vitro*. Prevented tumor growth *in vivo*, whereas tumor size increased five-fold after control peptide treatment.	24
Mammary carcinoma murine model	Aminopeptidase A (APA)	CPRECESIC	Inhibited APA enzymatic activity, suppressed endothelial cell migration and proliferation, and inhibited capillary tube formation *in vitro*. Suppressed neovascularization and inhibited tumor growth *in vivo*.	25
Breast cancer and melanoma xenografts in nude mice	Tumor and endothelial cell lymphatics	CGNKRTRGC	Induced apoptosis *in vitro*. Homed to tumors and metastatic lesions, inhibited tumor growth, and reduced tumor lymphatics *in vivo*.	26, 27
Small cell lung cancer and prostate cancer xenografts in nude mice	E2F-1 transcription factor	HHHRLSH	Conjugated to penetratin to facilitate cell uptake, peptide was cytotoxic to a range of tumor cells *in vitro*. Encapsulated in liposomes to increase serum stability, peptide inhibited tumor volume growth.	28, 29
Monovalent Peptide-Drug Conjugates				
Breast carcinoma xenograft in nude mice	Aminopeptidase N (APN), or CD13, in tumor vasculature	CDCRGDCFC-Dox and CNGRC-Dox (doxorubicin)	Tumor reduction by one-fourth to one-fifth the size of control treated tumors, fewer metastases, and longer survival relative to untargeted Dox	30
Lymphoma and melanoma in murine model	APN^{30}	CNGRCG-$TNF_{1–157}$	Efficacy:toxicity ratio 14 times greater than untargeted TNF. Similar pharmacokinetics as untargeted TNF.	31
Prostate cancer xenograft in nude mice	LNCaP cells	GTIQPYPFSWGY-$_D$(KLAKLAK)$_2$	Induced LNCaP cell death *in vitro*. Exhibited high biodistribution to tumors *in vivo*.	32
Colon carcinoma in murine model	Tumor-associated macrophages (TAMs)	YEQDPWGVKWWY GGGS-$_D$(KLAKLAK)$_2$	M2 macrophage specific binding and uptake *in vitro*. Delayed mortality and	33

Indication	Target	Targeting Peptide	Result	Ref
			selective elimination of TAMs *in vivo*.	
Multivalent Peptide Conjugates				
Non-small cell lung cancer xenografts in nude mice	$\alpha_v\beta_6$ integrin on H2009 cells[34]	RGDLATLRQLAQE DGVVGVR[35]	Greater affinity and serum stability of tetrameric peptides (relative to mono-, di-, and trimeric) to cells *in vitro*. Five-fold greater tumor-to-blood ratio for tetrameric peptides relative to scrambled control *in vivo*.	36
Non-small cell lung cancer xenografts in nude mice	Human NCI-H460 lung cancer cells	CRCPLSHSLICYC	Time- and dose-dependent uptake by lung cancer cells *in vitro*. Higher tissue distribution to xenografts relative to untargeted dendrimers *in vivo*.	37
Bladder carcinoma xenografts in nude mice	Carbohydrate-associated antigens on tumor cells[38]	SGPG[VG-SNRDARR-G-$(VGVPG_{12})$]$_5$	1.3-fold greater binding than monomeric SNRDARR and 17-fold greater binding than controls to bladder cancer cells *in vitro*. Time-dependent, 2.3-fold greater tumor accumulation relative to controls *in vivo*.	39
Breast carcinoma xenografts in nude mice	Interleukin-4 receptor[40]	[VG-RKRLDRN-G-$(VGVPG)_{12}$]$_6$	Binding to and uptake by breast carcinoma cells *in vitro*. Exerted cytotoxicity by blocking IL-4 receptors. Tumor tissue retention of at least 24 h *in vivo*.	41
Prostate cancer and breast cancer xenografts in nude mice	Clotted plasma proteins and fibrinogen[42] and Tumor lymphatics[27]	CREKA and CGNKRTRGC	Extravasation into tumor tissue (both prostate- and breast-derived tumors) *in vivo*.	43
Multivalent Peptide-Polymer Conjugates				
Melanoma metastasis to lung in murine model	E-selectin[44]	DITWAQLWDLMK	Binding to brain capillary endothelium cells *in vitro*. pH-sensitive hydrazide-mediated release of doxorubicin or $D(KLAKLAK)_2$ from 34 kDa copolymers prolonged survival.	45
Primary lung carcinoma and melanoma pulmonary metastases	Vascular Endothelial growth factor receptor-1 (VEGFR-1)[46]	WHSDMEWWYLLG	Binding to VEGFR-1 expressing endothelial cells *in vitro*. Tumor-specific doxorubicin delivery inhibited tumor growth and extended survival.	47

Indication	Target	Targeting Peptide	Result	Ref
Fracture in murine model	Tartrate-resistant acid Phosphatase (TRAP)[6]	TPLSYLKGLVTVG	Enhanced TRAP binding by random polymers relative to gradient polymers *in vitro*. Greater fracture persistence (at least one week) by 65 kDa random polymers.	48

Table 2:

Summary of multivalent nanoparticles (NPs) with phage-derived targeting peptides.

Indication	Target	Targeting Peptide	Nanostructure and size	Result	Ref
Post-assembly peptide conjugation					
Femur fracture in murine model	Tartrate-resistant acid phosphatase[6]	TPLSYLKGLV TVG	Micelle formation of PSMA-PS diblock copolymers by solvent exchange; carbodiimide peptide conjugation to form 50 nm micelles	Two-fold greater fracture accumulation relative to scrambled control *in vivo*. Fracture-specific drug delivery expedited healing and improved bone mechanical properties.	62
Liver-colonizing Colon 26 NL-17 cells in murine model	Human endothelial progenitor cells (hEPCs)	ASSHN	DPPC, CHOL, and DSPE-PEG_{2000}-MAL liposomes modified with ASSHNC peptide to form 101 nm particles	Intratumoral distribution *in vivo*. Tumor-specific doxorubicin delivery reduced tumor volume more than untargeted control.	63
Neuroblastoma xenografts in nude mice	APA[25] and APN[30]	CPRECES and CNGRC	Dual conjugation of peptides to HSPC, CHOL, DSPE-PEG_{2000}-NH_2 liposomes via BS3 cross-linker to form 90–115 nm liposomes	Superior tumor uptake of dual-targeted liposomes *in vivo*. Tumor-specific doxorubicin delivery led to tumor vasculature-associated endothelial cell and pericyte death and significantly greater life spans of mice.	64
Lung cancer xenografts in nude mice	Tumors responding to VEGF inhibitor treatment	HVGGSSV65	100 nm liposomes composed of DSPC, CHOL, and MAL-PEG_{2000}-DSPE modified with cysteine-functional peptide	Greater accumulation in irradiated tumors and time-dependent increase in doxorubicin delivery to tumors *in vivo*. Tumor-specific doxorubicin delivery induced apoptosis and delayed tumor growth.	66
Drug delivery through BBB	Brain	TGNYKALHP HNG	Cysteine-modified peptide conjugated to MAL-PEG-PLA micelles to form 110–120 nm particles	Uptake by brain-derived endothelial cells *in vitro*. High brain-to-liver and brain-to-spleen for TGN-NPs *in vivo*. Dye	67

Indication	Target	Targeting Peptide	Nanostructure and size	Result	Ref
				delivery to brain ~2- to 4-fold greater than controls.	
Breast carcinoma xenografts in nude mice, glioma murine model	Glucose-regulated protein GRP78	GIRLRG	Cysteine-modified peptide conjugated to allyl-functional poly(ester) NPs	Accumulation in irradiated tumors *in vivo*. Tumor-specific paclitaxel delivery resulted in 50% greater apoptosis and delayed tumor tripling time by 55 days.	68
Left carotid injury in rats	Human collagen IV	KLWVLPK	Cysteine-modified peptide conjugated to shell MAL-PEG-DSPE / core PLA-paclitaxel liposomes to form 60 nm particles.	Exhibited 10–12 day drug release and binding to injured aortas (percutaneous angioplasty) *in vitro*. Spatiotemporally control distribution to injured vessels *in vivo*.	69
Pre-assembly peptide conjugation					
Neuroblastoma, lung, ovarian, and prostate tumor xenografts in nude mice	APN[30]	CGNGRGGVR SSSRTPSDKY C	Peptide conjugated to DSPE-PEG_{2000}-MAL and combined with HSPC, CHOL, and DSPE-PEG_{2000} to form 90–115 nm liposomes	Dox-loaded NGR-liposomes exhibited high tumor uptake *in vivo*, tumor volumes were reduced, and mice achieved longer survival.	70–72
Glioblastoma xenograft in nude mice	VAV3 receptor[73]	SSQPFWS	MAL-PEG-PLA modified with SSQPFWSC peptides to form 23 nm micelles	High cellular uptake efficiency and tumor spheroid penetration *in vitro*. Tumor vasculature accumulation *in vivo*. Tumor-specific paclitaxel delivery inhibited tumor growth more than untargeted control.	74
Carotid artery ligation atherosclerosis murine model	Filamin-A in atheroprone regions of disturbed blood flow	GSPREYTSY MPH	Peptide conjugated to DPHE and combined with DPPC to form 64 nm liposomes	Five-fold greater accumulation in disturbed flow regions *in vivo*. Artery-specific BH4 delivery decreased superoxide concentration and reduced plaque burden.	75
Liver-colonizing Colon 26 NL-17 cells	Angiogenic vessels in dorsal air sac murine model	APRPG	Stearoyl-peptide combined with DSPC and CHOL to form 100 nm Liposomes	Binding to human islet cell and glioblastoma tumors *in vitro*.	76

Indication	Target	Targeting Peptide	Nanostructure and size	Result	Ref
and Meth A sarcoma in murine model				Time-dependent tumor accumulation *in vivo*. Tumor vessel-specific doxorubicin slowed tumor growth and increased life span.	
Carotid artery Ligation atherosclerosis murine model	Non-muscle myosin heavy chain IIA on endothelial cells in atheroprone vasculature	CLIRRTSIC	Peptide conjugated to NHS-PEG-MAL, then MAL reacted with disulfide-Crosslinked branched PEI. Complexed with siRNA to form 200 nm polyplexes	Binding to endothelial cells exposed to oscillatory shear stress *in vitro*. Selective binding to and gene knockdown in regions of disturbed flow *in vivo*.	77
RIP-Tag2 transgenic pancreatic cancer murine model	Pancreatic islet tumor[78], Potentially Frizzled-5 Receptor	CKAAKN	Peptide conjugated to 6-(maleimidyl)-Hexanoic acid(trisnor-squalenylidene)-hydrazide. SQ-CKAAKN mixed with SQ-gemcitabine to form 130–170 nm NPs	Binding to secreted frizzled related protein-4 and low complement activation *in vitro*. Tumor-specific gemcitabine delivery reduced tumor burden by 30% and vessel area by 60% compared to untargeted.	79
Gene delivery to the brain	Brain[67]	TGNYKALHP HNG	Peptide conjugated to MAL-PEG-pDMAEMA. Complexed with DNA to form 80 nm micelles	Uptake by brain capillary endothelial cells *in vitro*. Brain-specific DNA delivery qualitatively enhanced gene expression in the brain relative to untargeted.	80

Table 2 Abbreviations: APA, Aminopeptidase A. APN, Aminopeptidase N. BBB, Blood-brain barrier. BH4, Tetrahydrobiopterin. BS3, bis(sulfosuccinimidyl)suberate. CD, Cluster of differentiation. CHOL, Cholesterol. DOTAP, 1,2-dioleoyl-3-trimethylammonium-propane. DPHE, 1,2-dipalmitoyl-*sn*-glycero-3-phosphoethanolamine-N-hexanoylamine. DPPC, Dipalmitoylphosphatidylcholine. DPPG, 1,2-dipalmitoyl-*sn*-glycero-3-[phospho-*rac*-(1-glycerol)]. DSPC, 1,2-distearoyl-*sn*-glycero-3-phosphocholine. DSPE, 1,2-distearoylphosphatidylethanolamine. ePC, L-α-phosphatidylcholine. HSPC, Hydrogenated soybean phosphatidylcholine. MAL, Maleimide. MCF, Michigan Cancer Foundation. NHS, N-hydroxysuccinimide. pDMAEMA, poly(2-(dimethylamino) ethyl methacrylate). PE, 1,2-distearoyl-*sn*-glycero-3-phosphoethanolamine. PEG, poly(ethylene glycol). PEI, poly(ethyleneimine). PLA, poly(lactic acid). PSMA, poly(styrene-*alt*-maleic anhydride). PS, poly(styrene). SPDP, *N*-succinimidyl 3-(2-pyridyldithio)proprionate. SQ, squalene. VEGF, endothelial growth factor.